Inorganic Chemistry
Cite This: Inorg. Chem. XXXX, XXX, XXX−XXX
Article
pubs.acs.org/IC

Half-Sandwich Iridium(III) and Ruthenium(II) Complexes Containing P^P-Chelating Ligands: A New Class of Potent Anticancer Agents with Unusual Redox Features

JuanJuan Li, Meng Tian, Zhenzhen Tian, Shumiao Zhang, Chao Yan, Changfang Shao, and Zhe Liu*

Institute of Anticancer Agents Development and Theranostic Application, The Key Laboratory of Life-Organic Analysis and Key Laboratory of Pharmaceutical Intermediates and Analysis of Natural Medicine, Department of Chemistry and Chemical Engineering, Qufu Normal University, Qufu 273165, China

Supporting Information

ABSTRACT: A series of half-sandwich Ir^{III} pentamethylcyclopentadienyl and Ru^{II} arene complexes containing P^P-chelating ligands of the type $[(Cp^x/arene)M(P^P)Cl]PF_6$, where M = Ir, Cp^x is pentamethylcyclopentadienyl (Cp*), or 1-biphenyl-2,3,4,5-tetramethyl cyclopentadienyl (Cp^{xbiPh}); M = Ru, arene is 3-phenylpropan-1-ol (bz-PA), 4-phenylbutan-1-ol (bz-BA), or *p*-cymene (*p*-cym), and P^P is 2,20-bis(diphenylphosphino)-1,10-binaphthyl (BINAP), have been synthesized and fully characterized, three of them by X-ray crystallography, and their potential as anticancer agents explored. All five complexes showed potent anticancer activity toward HeLa and A549 cancer cells. The introduction of a biphenyl substituent on the Cp* ring for the iridium complexes has no effect on the antiproliferative potency. Ruthenium complex $[(\eta^6\text{-}p\text{-cym})Ru(P^P)Cl]PF_6$ (**5**) displayed the highest potency, about 15 and 7.5 times more active than the clinically used cisplatin against A549 and HeLa cells, respectively. No binding to 9-MeA and 9-EtG nucleobases was observed. Although these types of complexes interact with ctDNA, DNA appears not to be the major target. Compared to iridium complex $[(\eta^5\text{-Cp*})Ir(P^P)Cl]PF_6$ (**1**), ruthenium complex (**5**) showed stronger ability to interfere with coenzyme NAD^+/NADH couple through transfer hydrogenation reactions and to induce ROS in cells, which is consistent with their anticancer activities. The redox properties of the complexes **1**, **5**, and ligand BINAP were evaluated by cyclic voltammetry. Complexes **1** and **5** arrest cell cycles at the S phase, Sub-G_1 phase and G_1 phase, respectively, and cause cell apoptosis toward A549 cells.

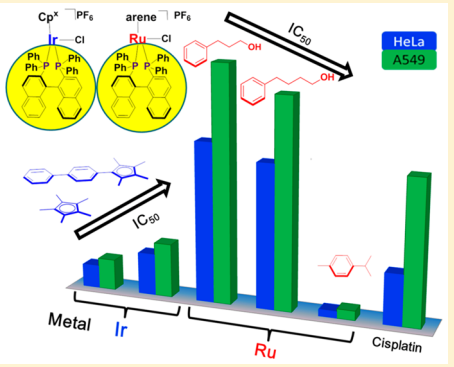

INTRODUCTION

Cisplatin is one of the earliest and most successful metal based anticancer drugs in the clinic, which is still used in cancer treatment after almost five decades since its chance discovery.[1] In the field of metal based anticancer agents, cisplatin is still the benchmark for evaluation of antiproliferative activity and comparison of mechanism of action.[2,3] However, due to the disadvantages of cisplatin and other platinum based anticancer drugs, such as dose-dependent side effects and the development of resistance of some carcinomas, a wide range of novel transition metal complexes that might be effective against a wider range of cancers, with less side effects and different mechanisms of action, are being screened for their use as therapeutic agents.[4−10]

Iridium (Ir) is a third-row transition metal, and its compounds are usually considered to be too inert to possess high activity. A few early trials seem to confirm this assumption.[11,12] However, very recently, iridium(III) complexes have been shown to possess great potential as novel anticancer agents, which not only showed high potency toward a wide range of cancer cells but also displayed completely different mechanisms of action (MOAs) from the clinically used platinum based drugs.[13−25] Sheldrick and co-workers reported a series of cytotoxic trichlorido or Cp* Ir^{III} complexes containing N^N-chelating polypyridyl ligands, such as *fac*-$[Ir(phen)(dmso\text{-}kS)Cl_3]$ (phen = 1,10-phenanthroline), which are highly active against MCF-7 human breast cancer cells and HT-29 human colon cancer cells.[26,27] The Sadler group started to explore iridium based anticancer agents in 2008. At the start, a series of Ir^{III} Cp* chlorido complexes containing N^N-, O^O-, or O^N-chelating ligands, such as $[(\eta^5\text{-Cp*})Ir(phen)Cl]PF_6$, were synthesized; however, the antiproliferative activity test showed that they were inactive (IC_{50}, concentration at which 50% of the cell growth is inhibited, >100 μM) against A2780 human ovarian cancer cells.[28] However, when a phenyl or biphenyl ring was introduced onto the Cp* ring, a significant increase in the anticancer activity against A2780 cells was achieved, for example, from $[(\eta^5\text{-Cp*})Ir(phen)Cl]PF_6$ (IC_{50} > 100 μM) to $[(\eta^5\text{-}Cp^{xbiph})Ir(phen)Cl]PF_6$ (Cp^{xbiph} = $C_5Me_4C_6H_4C_6H_5$) (IC_{50} = 0.72 μM).[28] Furthermore, Cp* complex $[(\eta^5\text{-Cp*})Ir(C^N)Cl]PF_6$, bearing an anionic C^N-chelating 2-phenylpyridine ligand, instead of a neutral diimine type ligand (such as phen and 2,2′-bipyridine), displayed

Received: July 31, 2017

DOI: 10.1021/acs.inorgchem.7b01959
Inorg. Chem. XXXX, XXX, XXX−XXX

promising anticancer activity, with IC_{50} value 10.8 μM against A2780 cell line.[29] Going from $[(\eta^5\text{-Cp*})Ir(C\text{^}N)Cl]PF_6$ to $[(\eta^5\text{-Cp}^{xbiph})Ir(C\text{^}N)Cl]PF_6$ (C^N = 2-phenylpyridine), an order of magnitude increase in potency, from IC_{50} 10.8 to 0.7 μM against A2780 cells, was achieved upon the inclusion of a biphenyl substituent to the Cp* ring.[30]

Ruthenium is another valuable metal in the search for therapeutic agents.[2] Ruthenium compounds are attracting much attention for anticancer drug design since they have a rich redox chemistry (Ru^{II} and Ru^{III}) and exhibit a similar spectrum of kinetics to platinum(II).[31] In general, ruthenium complexes show less toxicity than their platinum analogues, as ruthenium is able to mimic iron during its interaction with proteins, such as transferrin and albumin; thus, more selective entry into cancer tissues can be achieved as more transferrin receptors located on the cancer cell surface.[2,32,33] A large number of ruthenium compounds have been designed and displayed potent anticancer activities. Moreover, two ruthenium(III) complexes have entered clinical trials.[34−36] The Ru^{II} ethylenediamine (en) complexes developed by the Sadler group, $[(\eta^6\text{-arene})Ru(en)Cl]^+$, have been evaluated for activity both in vitro in A2780 cancer cells and in vivo, showing potent activity and non-cross-resistance to cisplatin-resistant cells.[37] Dyson et al. reported the high selectivity of an arene Ru^{II} PTA series of compounds (pta = 1,3,5-triaza-7-phosphatricyclo-[3.3.1.1]decane) toward the TS/A mouse adenocarcinoma cancer cells and HBL-100 human mammary normal cells.[38]

With regard to half-sandwich Ir^{III} and Ru^{II} complexes $[(Cp^x/arene)M(L\text{^}L')Z]^{0/n+}$, all of the ligands around the metal center including the cyclopentadienyl/arene, chelating ligand, L^L′, and leaving group Z can influence the anticancer activity dramatically.[4,15,18,39] Ru^{II} arene anticancer complexes, where arene, for example, is benzene, *p*-cymene (*p*-cym), biphenyl, 9,10-dihydroanthracene (DHA), and 5,8,9,10-tetrahydroanthracene (THA), have been widely investigated for the effects of various arenes on the chemical and biological activities.[40,41] A large number of metal complexes based on N^N-chelating ligands have been evaluated for their medicinal application, while complexes containing P^P-chelating ligands are much less investigated.[36,42−44] Only a few Ir^{III} complexes with P^S-chelating ligand show comparable or even higher antiproliferative activities than cisplatin against 8505C and SW480 cell lines.[45]

Metal complexes of 2,20-bis(diphenylphosphino)-1,10-binaphthyl (BINAP) have recently drawn attention as promising asymmetric catalyts in many organic reactions.[46] However, to the best of our knowledge, no biological activity of iridium or ruthenium BINAP complexes has been reported so far. In this work, a series of half-sandwich Ir^{III} and Ru^{II} complexes of the type $[(\eta^5\text{-Cp}^x)Ir(P\text{^}P)Cl]PF_6$, where Cp^x is pentamethylcyclopentadienyl Cp* (**1**), biphenyl (Cp^{xbiph}) derivatives (**2**), and $[(\eta^6\text{-arene})Ru(P\text{^}P)Cl]PF_6$, where the arene is 3-phenylpropan-1-ol (bz-PA) (**3**), 4-phenylbutan-1-ol (bz-BA) (**4**), and *p*-cymene (*p*-cym) (**5**), with BINAP as P^P-chelating ligand, were synthesized and characterized (Chart 1). We report studies of the nucleobase binding, DNA interactions, BSA interactions, and cell toxicity of the complexes. The work also explores the MoA of these metal complexes by cell cycle, ROS, apoptosis, and catalytic hydride transfer analysis. The results suggest that this series of metal complexes are potential candidates for development as new therapeutic agents.

Chart 1. Organometallic Ir^{III} Cyclopentadienyl $[(\eta^5\text{-Cp}^x)Ir(P\text{^}P)Cl]PF_6$ and Ru^{II} Arene $[(\eta^6\text{-arene})Ru(P\text{^}P)Cl]PF_6$ Complexes Studied in This Work

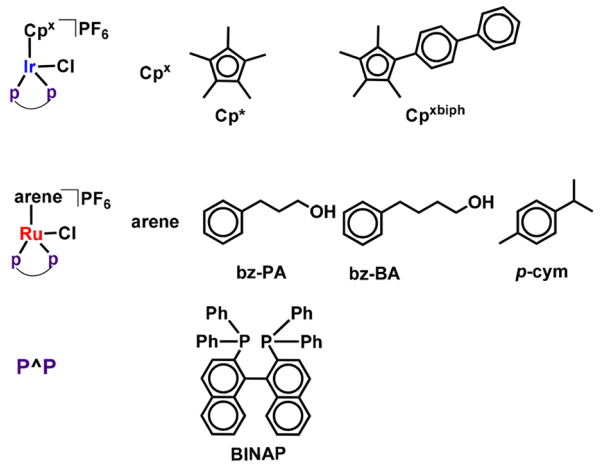

Complex	Metal	Cp^x/Arene	P^P
1	Ir	Cp*	BINAP
2	Ir	Cp^{xbiph}	BINAP
3	Ru	bz-PA	BINAP
4	Ru	bz-BA	BINAP
5	Ru	*p*-cym	BINAP

RESULTS AND DISCUSSION

The dinuclear dichloro-bridged complexes $[(\eta^5\text{-Cp*})IrCl_2]_2$ (**dimer 1**) and $[(\eta^5\text{-Cp}^{xbiph})IrCl_2]_2$ (**dimer 2**) were synthesized by microwave heating of $IrCl_3$ and relative cyclopentadienyl ligand in absolute methanol.[18] Dimeric μ-chloro-bridged complexes $[(\eta^6\text{-bz-PA})RuCl_2]_2$ (**dimer 3**), $[(\eta^6\text{-bz-BA})RuCl_2]_2$ (**dimer 4**)[47] and $[(\eta^6\text{-}p\text{-cym})RuCl_2]_2$ (**dimer 5**)[48] are readily formed upon conversion of 3′-(2,5-dihydrophenyl)propanol, 4′-(2,5-dihydrophenyl)butanol,[49] and α-terpinene, respectively, with $RuCl_3$ under refluxing in absolute methanol (Scheme 1). Complexes **1**−**5** were synthesized by reactions between the ligand BINAP and the dinuclear iridium/ruthenium precursors **dimers 1**−**5** in methanol at ambient temperature. All complexes are newly synthesized compounds and were characterized by ^1H NMR, mass spectroscopy, and elemental analysis. All complexes were isolated as PF_6^- salts.

X-ray Crystal Structures. Single crystals of $[(\eta^5\text{-Cp*})Ir(P\text{^}P)Cl]PF_6$ (**1**), $[(\eta^6\text{-bz-PA})Ru(P\text{^}P)Cl]PF_6$ (**3**), and $[(\eta^6\text{-}p\text{-cym})Ru(P\text{^}P)Cl]PF_6$ (**5**) were grown by slow diffusion of hexane into a saturated dichloromethane solution of these complexes. The structures and their atom numbering schemes are shown in Figure 1. Crystallographic data and selected bond lengths and angles are listed in Tables 1 and 2. Complexes of **1**, **3**, and **5** are arranged in the triclinic and monoclinic crystal systems with the $P\bar{1}$, $P2_1/n$, $C2/c$ space groups, respectively. Each complex has the expected pseudo-octahedral half-sandwich piano stool geometry. The distance between the iridium center and the centroid of η^5-cyclopentadienyl ring is 1.913 Å, while the distances between the ruthenium center and the centroid of η^6-arene for complexes **3** and **5** are 1.760 and 1.799 Å, respectively. The three complexes have similar metal−Cl bond distances for **1**, **3**, and **5**: 2.3922(17), 2.384(3), and 2.391(3) Å, respectively. The Ir−P bond lengths in **1** are similar

DOI: 10.1021/acs.inorgchem.7b01959
Inorg. Chem. XXXX, XXX, XXX−XXX

Scheme 1. Synthesis of dimers 3−5 and Respective Half-Sandwich Ir^{III} and Ru^{II} Complexes

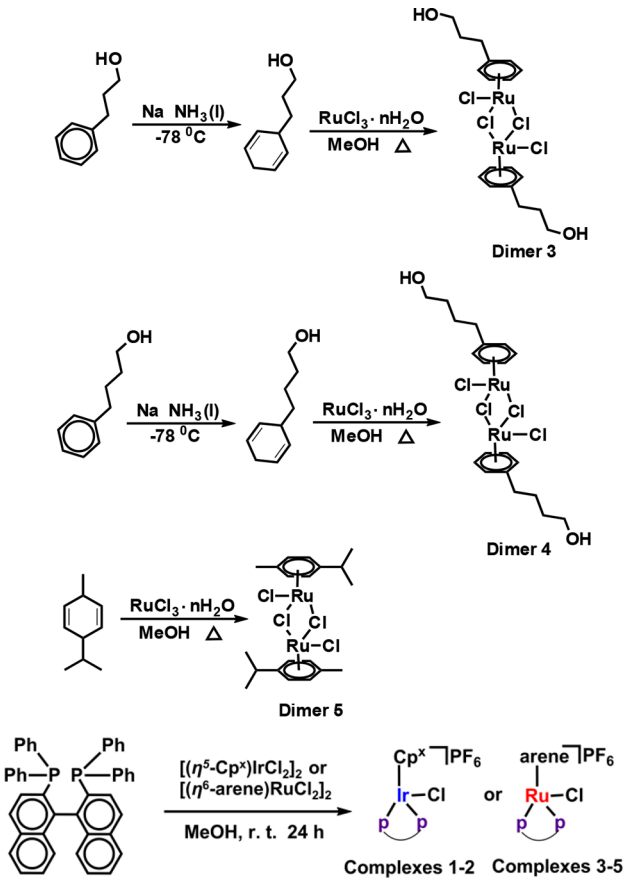

to the Ru−P bond lengths in **3** and **5**. However, slight differences between the metal−P_1 and metal−P_2 distances were observed in all three complexes (Table 2).

Comparison between the η^6-arene in complexes **3** and **5** shows that the functionalized arene in complex **3** is closer to the Ru^{II} center. This could be due to the presence of the stronger electron-donating group OH in addition to the steric hindrance effect of the isopropyl group. Due to the relatively strong trans effect of the P^P-chelating ligand BINAP, the Ir-centroid bond length 1.913 Å in complex **1** is significantly longer than the 1.820 and 1.786 Å found in the C^N complex [(η^5-Cp*)Ir(phpy)Cl] and the N^N complex [(η^5-Cp*)Ir-(bpy)Cl]Cl, respectively.[28,29,50] The Ir−Cl bond length 2.3922(17) Å in complex **1** is similar to the Ir−Cl bond length 2.3968(7) Å in [(η^5-Cp*)Ir(phpy)Cl] and 2.404(2) Å in [(η^5-Cp*)Ir(bpy)Cl]Cl.

Cytotoxicity. The aim of the present study is to investigate the in vitro viability of HeLa human cervical and A549 human lung cancer cell lines after treatment with various concentrations of complexes **1**−**5** over 24 h. The potentials of the synthesized complexes **1**−**5** on the IC_{50} values (concentration at which 50% of the cell growth is inhibited) after 24 h of exposure to the compounds are listed in Table 3. The HeLa cells and A549 cells were treated with cisplatin in the same concentration range and used as a control, and they showed an IC_{50} value of 7.5 μM toward HeLa cancer cells and 21.3 μM toward A549 lung cancer cells, respectively. Excitingly, the newly synthesized five complexes exhibited potency at least comparable to cisplatin against A549 cells with IC_{50} values ranging from 1.4 to 35.0 μM, and against HeLa cells with IC_{50} values from 1.0 to 23.7 μM. The activities of complexes **1**−**5** fall in the following order **5** > **1** > **2** > cisplatin > **4** > **3** toward both HeLa and A549 cancer cells. Against our expectations,[28] the Cp* complex **1** exhibited an antiproliferative activity 2 times higher toward both cell lines than its Cp^{xbiph} analogue **2**. This result is contrary to our previous conclusions, which showed the anticancer activity increased significantly with an increase in the number of phenyl rings on the Cp* ring.[4] The presence of the extended phenyl rings not only increased the hydrophobicity of the complexes, thereby easing their passage through the cell membrane so that more complex could find its way into the cells, but also had the potential for intercalation into DNA base pairs. The result here may be indicating that the presence of arenes in the chelating ligand BINAP may have offset the advantages of having the extended arenes on the Cp*. Complex **1** containing Cp* showed similar activity compare to [(η^5-Cp*)Ir(N^O)Cl]PF_6 (N^O = 1,2-naphthoquinone-1-oximato) against HeLa cells.[51] Sheldrick and co-workers reported a series of cytotoxic Cp* Ir^{III} complexes containing N,N-chelating polypyridyl ligands. In general, the antiproliferative effects of this type of N,N-bound polypyridyl Ir^{III} complexes are governed by the size of the polypyridyl ligands in the order of bpy < phen, dpq < dppz < dppn.[52]

Ruthenium complex **5** displayed the most potent antiproliferative activity against both cell lines: about 15 and 7.5 times more potent than cisplatin toward A549 and HeLa cells, respectively. Ruthenium complexes **3** and **4** containing the −OH group are less active, probably due to the hydrophilicity of −OH, and therefore noneffective in penetrating into the cell membrane.[53] From complex **3** to **4**, the antiproliferative activity improved slightly with the increase of ligand length of the backbond. Sadler et al. reported that the more hydrophobic the arene ligand is, the better cancer cell growth inhibitory activity.[37] Kim's group also reported a similar trend in the in vitro anticancer activity of Ir(III), Rh(III), and Ru(II) complexes against the lymphoma cell line.[54]

For the most potent two complexes **1** and **5**, their antiproliferative activities were further evaluated against two human bronchial epithelial normal cells 16HBE and BEAS-2B (Table 3). Unfortunately, no selectivity was observed for the two complexes between cancer cells versus normal cells. Hence, more structural modification is necessary to improve the selectivity in future work.

Partition Coefficients (log *P*). Lipophilicity is often consistent with the cellular uptake efficiencies of chemotherapeutic agents, and therefore, it has significant effects on their cytotoxic potency. The log *P* values for complexes **1** and **5** in octanol/water systems were determined because of their low IC_{50} values. NaCl (50 mM) was used to suppress hydrolysis of the complexes so the log *P* values tested are for the chlorido complexes. The values of log *P* for **1** (2.04) and **5** (1.36) are varied with the metals and cyclopentadienyl or arene of the complexes (Table 4). The log *P* values of new pharmacophores in the Comprehensive Medicinal Chemistry database range from −0.4 to 5.6.[55] The log *P* values for complexes **1** and **5** are within this range. The hydrophobicity and anticancer activity were not correlated in this study. Complex **5** displays lower hydrophobicity but the most cytotoxic activity.

Nucleobases Binding. As DNA is usually an important target for metal based anticancer compounds, the interaction between nucleobase models 9-ethylguanine (9-EtG) and 9-methyladenine (9-MeA) and complexes **1**−**5** was investigated.

DOI: 10.1021/acs.inorgchem.7b01959
Inorg. Chem. XXXX, XXX, XXX−XXX

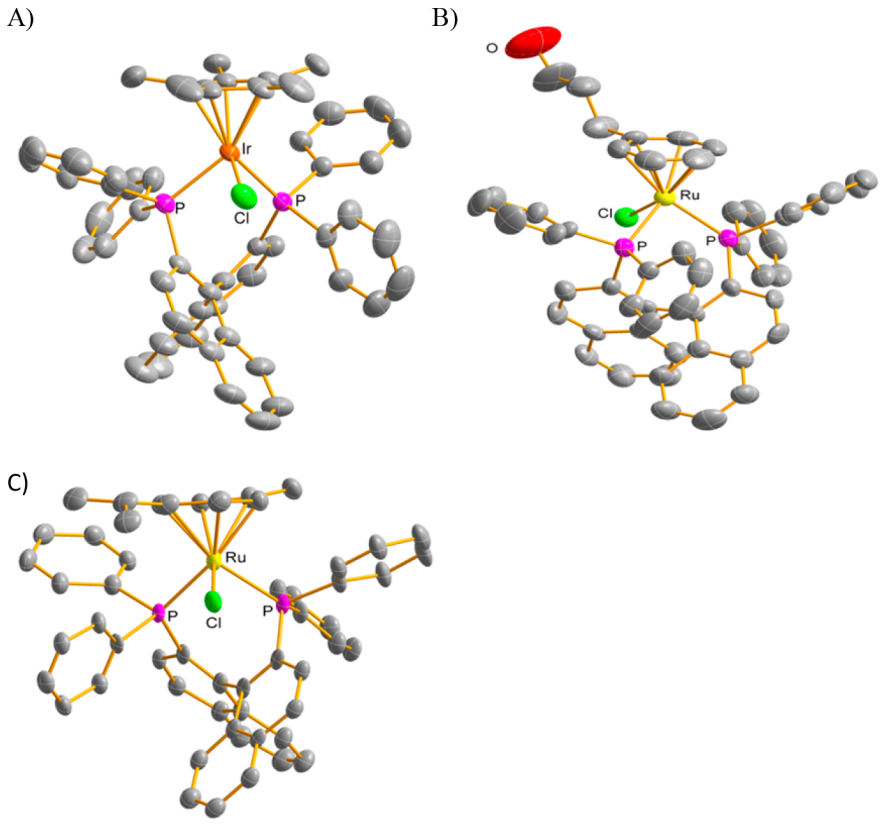

Figure 1. X-ray crystal structures for (A) $[(\eta^5\text{-Cp*})\text{Ir(P^P)Cl}]\text{PF}_6$ (**1**), (B) $[(\eta^6\text{-bz-PA})\text{Ru(P^P)Cl}]\text{PF}_6$ (**3**), and (C) $[(\eta^6\text{-}p\text{-cym})\text{Ru(P^P)Cl}]\text{PF}_6$ (**5**). Hydrogen atoms, solvent CH_2Cl_2, and counterions PF_6^- are omitted for clarity.

Table 1. Crystallographic Data for $[(\eta^5\text{-Cp*})\text{Ir(P^P)Cl}]\text{PF}_6$ (1), $[(\eta^6\text{-bz-PA})\text{Ru(P^P)Cl}]\text{PF}_6$ (3), and $[(\eta^6\text{-}p\text{-cym})\text{Ru(P^P)Cl}]\text{PF}_6$ (5)

	1	3	5
formula	$C_{54}H_{47}ClF_6IrP_3$	$C_{53}H_{44}ClF_6OP_3Ru$	$C_{56}H_{50}Cl_5F_6P_3Ru$
MW	1130.48	1040.31	1208.19
Cryst size (mm)	0.42 × 0.35 × 0.30	0.20 × 0.12 × 0.08	0.30 × 0.20 × 0.12
λ (Å)	0.71073	0.71073	0.71073
temp (κ)	298(2)	293(2)	298(2)
cryst syst	Triclinic	Monoclinic	Monoclinic
space group	$P\bar{1}$	$P21/n$	$C2/c$
a (Å)	12.2960(11)	16.296(2)	33.150(3)
b (Å)	12.7308(12)	18.704(3)	15.2970(14)
c (Å)	15.3989(14)	16.701(2)	21.6051(19)
α (deg)	77.0650(10)	90	90
β (deg)	86.567(2)	110.879(3)	99.1530(10)
γ (deg)	85.275(2)	90	90
vol (Å^3)	2339.2(4)	4756.3(11)	10816.4(16)
Z	2	4	8
R1 [$I > 2\sigma(I)$]	0.0506	0.0948	0.1264
wR2 [$I > 2\sigma(I)$]	0.1294	0.2319	0.3086
GOF	1.043	0.948	1.048

9-MeA or 9-EtG (3 mol equiv) was added to a solution of **1**−**5** (1.0 mM) in 80% DMSO-d_6/20% D_2O (v/v) at 310 K. No additional ^{1}H NMR peaks were detected over 24 h (Figure S1 in the Supporting Information). Also, no adducts formation was detected by mass spectrometry.

Interaction with GSH. GSH is plentiful in cells and participates in the detoxification of many anticancer drugs.[15] Therefore, we investigated the stability of complexes **1** and **5** in the absence and presence of GSH due to their high anticancer potency. ^{1}H NMR spectra showed that no hydrolysis was observed for complexes **1** and **5** in 80% DMSO-d_6/20% D_2O (v/v) after 24 h at 310 K (Figure S2 in the Supporting Information). DMSO was used to ensure solubility of metal complexes in solution. Then GSH (5 mol equiv) was added to the solution under N_2 atmosphere. The resulting solution was monitored by ^{1}H NMR at 310 K. No adduct of complexes and GSH was detected after 2 h, suggesting that the iridium/ruthenium chloride complexes are stable in the absence and

DOI: 10.1021/acs.inorgchem.7b01959
Inorg. Chem. XXXX, XXX, XXX−XXX

Table 2. Selected Bond Lengths (Å) and Angles (deg) for $[(\eta^5\text{-Cp*})Ir(P\text{^}P)Cl]PF_6$ (1), $[(\eta^6\text{-bz-PA})Ru(P\text{^}P)Cl]PF_6$ (3), and $[(\eta^6\text{-}p\text{-cym})Ru(P\text{^}P)Cl]PF_6$ (5)

	1	3	5
M−C (cyclopentadienyl)	2.242(7)	2.182(12)	2.231(15)
	2.250(7)	2.228(12)	2.262(15)
	2.259(7)	2.248(12)	2.265(18)
	2.272(7)	2.249(12)	2.31(2)
	2.324(6)	2.266(12)	2.330(17)
		2.304(11)	2.330(17)
M−C(centroid)	1.913	1.760	1.799
$M-P_1$	2.3272(16)	2.365(3)	2.333(4)
$M-P_2$	2.3522(17)	2.338(3)	2.391(4)
M−Cl	2.3922(17)	2.384(3)	2.391(3)
P_1-M-P_2	91.72(6)	91.15(10)	90.53(13)
P_1-M-Cl	85.59(6)	88.31(10)	84.70(12)
P_2-M-Cl	91.23(6)	85.88(10)	89.28(13)

presence of GSH, which may avoid deactivation too early before reaching their targets.

Interaction with ctDNA. The experiment was carried out keeping the concentration of complexes **1**−**5** constant (3.33 μM) and increasing the concentration of ctDNA (0−0.3 mM), and the reaction solution was monitored by UV−vis spectroscopy (Figure 2, Figure S3 in the Supporting Information, and Table 5). Addition of increasing amounts of ctDNA results in hypochromism at 214−220 nm and moderate bathochromic shift (3−6 nm) for all complexes, indicating a significant interaction with ctDNA, probably due to noncovalent binding modes of electrostatic binding and/or intercalations between base pairs.[56,57] Intercalation into DNA by complexes often causes bathchromism and hypochromism due to strong stacking interaction between aromatic chromophore and base pairs of DNA. Compared to the iridium complexes **1** and **2**, ruthenium complexes **3**−**5** caused more significant hypochromism.

Interactions of the complexes with ctDNA were fitted to the Benesi−Hildebrand equation (eq 1) to calculate the binding constants K_b[58]

$$\frac{A_0}{(A-A_0)} = \frac{\varepsilon_f}{(\varepsilon_b-\varepsilon_f)} + \frac{\varepsilon_f}{K_b(\varepsilon_b-\varepsilon_f)[DNA]} \quad (1)$$

where ε_b and ε_f are the extinction coefficients of the complex in bound and free form, respectively; A_0 is the initial absorbance of free complex, and A is the absorbance of the compound in the presence of DNA. The plot of $A_0/(A-A_0)$ versus 1/[DNA] gives a straight line, and the binding constants (K_b) were calculated as slope/intercept ratio (Figure 2 inset and Figure S3 inset in the Supporting Information).

Table 4. Log *P* for Complexes 1 and 5[a]

complex	log *P*
	Mean
1	2.04 ± 0.12
5	1.36 ± 0.07

[a]Results are obtained from three independent experiments.

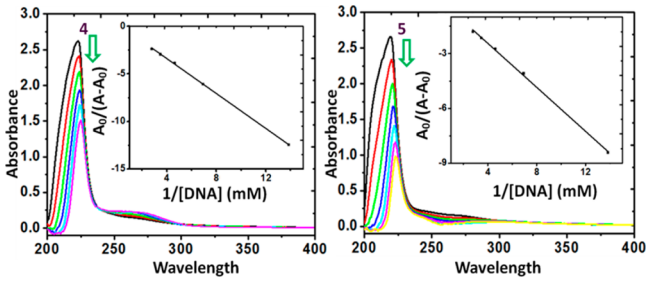

Figure 2. UV−vis spectra of complexes **4** and **5** (3.33 μM) upon addition of ctDNA (0−0.3 mM) in 5 mM Tris−HCl/10 mM NaCl buffer solution (pH = 7.2). The arrows show the direction of change in absorbance upon increasing the concentration of the complex. Inset: Plot of $A_0/(A-A_0)$ vs 1/ [DNA].

Table 5. Absorption Spectroscopic Properties of the Ir^{III}/Ru^{II} Complexes on Binding to DNA

Complex	Absorption λ_{max} (nm)		$\Delta\lambda$	Hypochromicity (%)	K_b (M^{-1})
	Free	Bound[a]			
1	215	218	3	22.0	6.4×10^4
2	214	219	5	21.0	3.1×10^3
3	218	224	6	44.1	1.6×10^4
4	223	225	2	42.5	4.1×10^3
5	219	223	4	45.9	3.6×10^4

[a][M] = 3.33 μM at [DNA]/[M] = 90.

As the four complexes have the same P^P-chelating ligand and overall charge on the complex, the difference between binding constants is mainly related to the nature of the cyclopentadienyl/arene ring and the metal ions. In general, iridium complexes showed higher binding constants K_b than ruthenium complexes, and Ir Cp* complex **1** displayed the highest K_b to ctDNA in the four complexes tested. Sadler and co-workers have previously reported that Cp^{xbiph} complexes displayed a much higher intercalative ability compared to their Cp* analogues.[28] However, in comparison with **1**, substitution of the methyl group with biphenyl decreases the K_b from 6.4×10^4 M^{-1} to 3.1×10^3 M^{-1} (**2** vs **1**). The introduction of functionalized ligand *p*-cym analogue increases the value of K_b

Table 3. In Vitro Anticancer Activity of Complexes 1−5 toward A549 and HeLa Cancer Cells and 16HBE and BEAS-2B Normal Cells over 24 h

Complex	IC_{50} (μM)			
	A549	HeLa	16HBE	BEAS-2B
$[(\eta^5\text{-Cp*})Ir(P\text{^}P)Cl]PF_6$ (**1**)	4.6 ± 0.1	3.4 ± 0.5	2.4 ± 0.1	2.8 ± 0.1
$[(\eta^5\text{-Cp}^{xbiph})Ir(P\text{^}P)Cl]PF_6$ (**2**)	8.0 ± 0.1	6.2 ± 0.3		
$[(\eta^6\text{-bz-PA})Ru(P\text{^}P)Cl]PF_6$ (**3**)	35.0 ± 1.1	23.7 ± 1.5		
$[(\eta^6\text{-bz-BA})Ru(P\text{^}P)Cl]PF_6$ (**4**)	31.1 ± 3.4	21.4 ± 2.5		
$[(\eta^6\text{-}p\text{-cym})Ru(P\text{^}P)Cl]PF_6$ (**5**)	1.4 ± 0.1	1.0 ± 0.1	1.3 ± 0.1	1.3 ± 0.1
Cisplatin	21.3 ± 1.7	7.5 ± 0.2		

DOI: 10.1021/acs.inorgchem.7b01959
Inorg. Chem. XXXX, XXX, XXX−XXX

by approximately 2.3 times compared to the 3-phenylpropan-1-ol (**5** vs **3**) and about 9 times compared to the 4-phenylbutan-1-ol.

Reaction with NADH. In a wide range of biocatalyzed processes, coenzyme nicotinamide adenine dinucleotide NADH and its oxidized form NAD^+ play crucial roles. Sadler and co-workers have reported that aqua Ir^{III} cyclopentadienyl complexes can catalytically convert NADH to NAD^+ and can produce ROS H_2O_2 and thus offer an oxidant pathway.[15,59] Therefore, reactions between metal complexes **1**−**5** and NADH were investigated. First, complexes **1** and **5** were chosen again because of their low IC_{50} values and their reactions with NADH were monitored by ^1H NMR. Mixed CD_3OD-d_4 and D_2O (v/v 2:1) was used to enhance the solubility of Ir^{III}/Ru^{II} complexes. When NADH (5 mol equiv) was added to the above solution of complexes **1** and **5** (1 mM), new peaks at 8.9, 9.3, and 9.5 ppm corresponding to NAD^+ were observed, which indicates NADH was converted into its oxidized form NAD^+. Interestingly, a singlet peak at −12.1 and −0.8 ppm, corresponding to the Ru−H and Ir−H hydride peaks, respectively, was observed after 2 h (Figure 3A and Figure S4 in the Supporting Information). Second, we investigated whether these complexes could catalytically convert NADH to NAD^+. Complexes **1**−**5** (1 μM) and NADH (100 μM) were mixed in 50% MeOH/50% H_2O (v/v) and monitored by UV−vis at 298 K (Figure 3B and Figure S6 in the Supporting Information). To evaluate the actual catalytic activity, we incubated the 100 μM NADH in a 50% MeOH/50% H_2O (v/v) solution as the control experiments (Figure S5 in the Supporting Information). As NADH has a UV absorption at 339 nm while its oxidized form NAD^+ has not, the turnover numbers (TONs) of complexes **1** (4.1), **2** (4.1), **3** (5.6), **4** (6.2), and **5** (15.5) were calculated by measuring the intensity changes at 339 nm (Figure 3B and Figure S6 in the Supporting Information). Ruthenium complex **5** possesses the highest TON among the four complexes, which is consistent with the most potent anticancer activity of **5**.

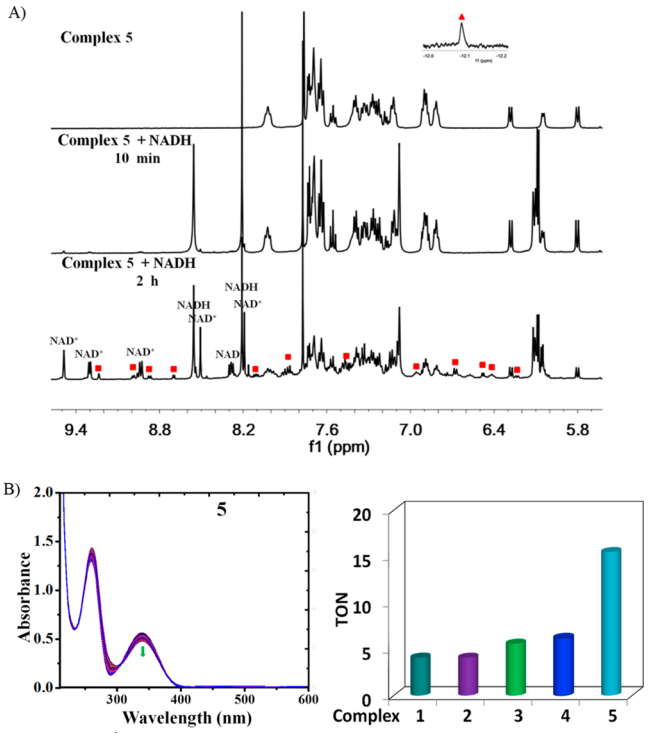

Figure 3. (A) ^1H NMR spectra showing reaction of complex **5** (1 mM) in 67% CD_3OD-d_4 and 33% D_2O (v/v) with NADH (5 mol equiv) at 310 K after 10 min and 2 h. Peaks labeled correspond to newly formed Ru−H complex. Inset: the generated Ru−H hydride peak (−12.1 ppm). (B) Left: conversion of NADH (100 μM) to NAD^+ by complex **5** (1 μM) in 50% MeOH/50% H_2O (v/v) recorded by UV−vis at 298 K for 9 h. Right: TONs of complexes **1**−**5**.

We showed that the Ir^{III} cyclopentadienyl and the Ru^{II} arene complexes catalyzed the NAD^+/NADH hydride transfer reactions effectively. Rh^{III} derivative can drive enzymatic reactions relying on NADH as a cofactor.[60] The large downfield shift of the Ir−H peak in $[(\eta^5\text{-Cp*})Ir(P\text{^}P)H]^+$ is notable compared to −11.1 ppm for $[(\eta^5\text{-Cp*})Ir(phen)(H)]^+$.[61] The TON of complex **5** (15.5) is about 2 times that of the half-sandwich Ir^{III} C^N-bound phenylpyridine complex and is much lower than that of the Ir^{III} N^N complex (max. 75).[15,18] The good catalytic performance may offer a pathway to the induction of ROS and a redox based MoA.

Electrochemical Properties. We performed cyclic voltammetry to further investigate the redox properties of the ligand BINAP and complexes **1** and **5** due to their low IC_{50} values in DMSO (Figure 4 and Figure S7 in the Supporting Information). All complexes were subject to two consecutive scans from 2 to −3 V at a scan rate of 100 mV/s. The two complexes showed similar electrochemical characteristics, and three irreversible reduction processes arose at reduction wave potentials of −2.10, −1.32, and 0.15 V for complex **1** and at −2.00, −1.33, and 0.16 V for complex **5** (Figure 4). The electrochemical data show that complexes with the same p^p ligands have similar CV behaviors. Comparison of the cyclic voltammograms of complexes **1** and **5** and ligand BINAP indicates that the three irreversible waves of complexes **1** and **5** may be assigned to the reduction of the p^p ligand and that the ancillary ligand BINAP has a significant effect on the electronic properties of these complexes.

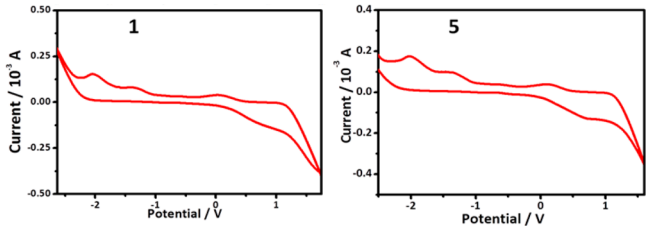

Figure 4. Cyclic voltammograms of complexes **1** and **5** in anhydrous DMSO solutions (1 mM), scan rate = 100 mV/s.

Apoptosis Assay. The two most promising complexes with low IC_{50} values, **1** (iridium) and **5** (ruthenium), are selected to carry out further investigations in order to shed light on their mechanism of action. Apoptosis is a means of programmed cell death. A great deal of metal based anticancer complexes inhibit cell growth via an apoptosis pathway.[62] In this work, we tried to investigate whether the cytotoxicity of the complexes **1** and **5** is due to apoptosis. A549 cancer cells were treated by the two complexes at concentrations of 0.5, 1, 2, and 3 × IC_{50} for 24 h. Annexin V and propidium iodide were used as stain agents, and the treated cells were analyzed by flow cytometry. After 24 h, complex **1** at a concentration of 0.5 × IC_{50} caused 9.7% and 15.1% of A549 cells in early apoptosis and late apoptosis, respectively (Figure 5 and Table S1 in the Supporting

DOI: 10.1021/acs.inorgchem.7b01959
Inorg. Chem. XXXX, XXX, XXX−XXX

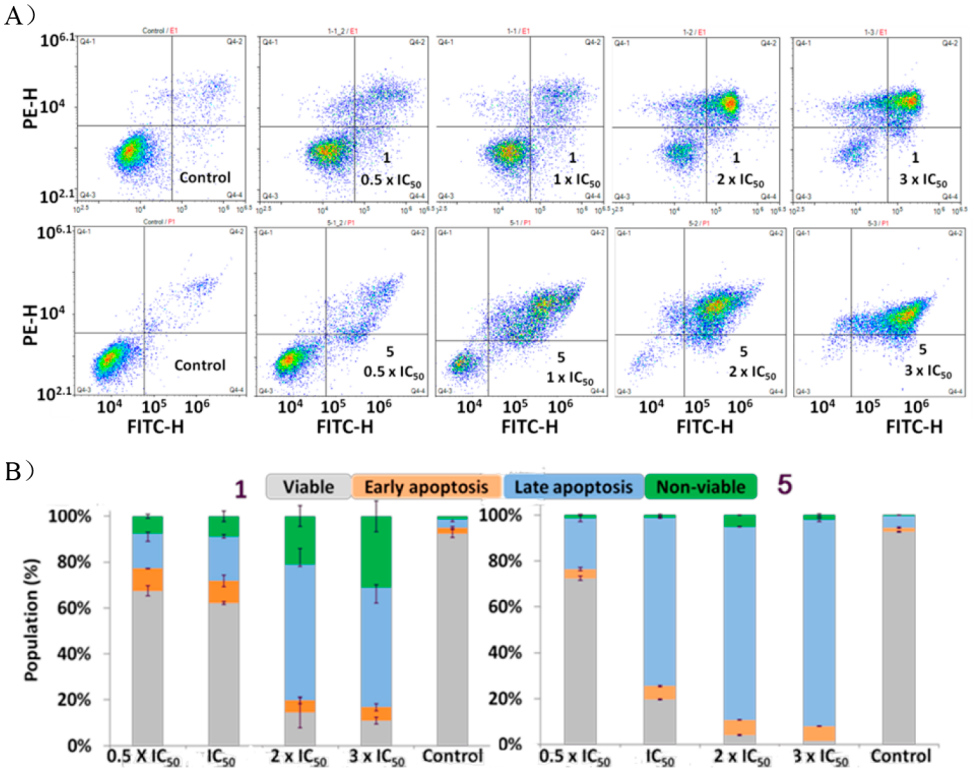

Figure 5. Apoptosis of A549 cancer cells induced by complexes **1** and **5** (concentrations used: 0.5, 1, 2, and 3 × IC_{50}) after 24 h at 310 K. Control: cells untreated. (A) Apoptotic cell death examined by flow cytometry. (B) Bar chart showing cell populations in various phases.

Information). At 3 × IC_{50}, cells in an apoptotic phase (early apoptosis + late apoptosis) increased to 57.9%. Interestingly, the ruthenium complex **5** displayed a much stronger ability to induce apoptosis than iridium **1**, where 79.1% of A549 cells were in apoptosis at IC_{50} and 96.5% at 3 × IC_{50}. This result is consistent with their antiproliferative performance. The results suggested that cell death caused by the complexes was induced mainly through apoptosis.

Cell Cycle Analysis. Next the effect of complexes **1** and **5** on cell cycle was studied by flow cytometry at 0.25 and 0.5 × IC_{50} of **1** and **5** over 24 h (Figure 6, Table S2 in the Supporting Information). Upon exposure of the A549 cells to **1** at concentration of 0.5 × IC_{50}, the percentages of cells in the S and Sub-G_1 phase increased 4.5% and 6.7%, respectively, suggesting cell cycle disturbing at the S and Sub-G_1 phase. The obviously dose-dependent increased subdiploid peak usually correlated to apoptosis (Figure 6A). For complex **5**, the percentages of cells in the G_1 phase of the cell cycle increased from 52.7% to 64.6% at concentration 0.5 × IC_{50}, suggesting an obvious cell cycle arrest at the G_1 phase. In addition, a slight apoptosis was observed as reflected by the small subdiploid peak (Figure 6A) for complex **5** at 0.5 × IC_{50}.

ROS Induction. Excessive generated reactive oxygen species (ROS) often cause cell damage.[15,63] In order to examine the ROS levels in A549 cancer cells induced by complexes **1** and **5**, flow cytometry analysis was performed (Figure 7, Table S3 in the Supporting Information). The ROS levels were found to be significantly increased in cells upon exposure to **1** and **5** for 24 h. Even at 0.25 × IC_{50}, about 68% and 86% of A549 cells were at high ROS levels after exposure to **1** and **5**, respectively (Figure 7). Ruthenium complex **5** is a stronger ROS inducer than the iridium complex **1**. This result correlates well with their antiproliferative behavior. These observations are consistent with the proposed MoA for **1** and **5**, which is based on the disruption of the cellular redox balance.[64] The dramatically increased ROS levels contributed to the killing of cancer cells.

The increased ROS levels in cells by complexes **1** and **5** may be related to the catalytic conversion of NADH to NAD^+. Sadler and co-workers have previously reported the possible chemical mechanisms of induction of ROS induced by iridium complexes, involving catalytic hydride transfer from NADH to iridium complexes to form iridium−hydride complexes and finally to oxygen to produce the ROS H_2O_2 as a product.[15]

■ CONCLUSION

This work seems to be the first report of organometallic iridium and ruthenium anticancer complexes containing BINAP as P^P-chelating ligand. We have studied here the effects on the chemical and anticancer activities by varying the Cp^x and η^6-arene ligand in $[(\eta^5\text{-}Cp^x)Ir(P\text{^}P)Cl]PF_6$ or $[(\eta^6\text{-arene})Ru(P\text{^}P)Cl]PF_6$. Three X-ray crystal structures were determined.

Complexes **1**−**5** displayed from promising to highly potent antiproliferative activity toward HeLa and A549 cancer cells (Figure 8). Ruthenium complex **5** is the best candidate and is 15 times more potent than clinically used cisplatin toward A549 cells. The anticancer activity can be fine-tuned by changing both metals and the cyclopentadienyl/arene ligands, in the order of Cp* > Cp^{xbiph} and *p*-cym > bz-BA > bz-PA.

Although interaction with ctDNA was observed, DNA possibly is not the main target. The complexes are effective catalysts for the oxidation of NADH to NAD^+ using NADH as the hydride source. This may induce ROS in cells. Indeed, complexes **1** and **5** increased ROS levels significantly in A549 cells even at low concentration. In addition, the metal complexes **1** and **5** disturbed the cell cycle at the Sub-G_1

DOI: 10.1021/acs.inorgchem.7b01959
Inorg. Chem. XXXX, XXX, XXX−XXX

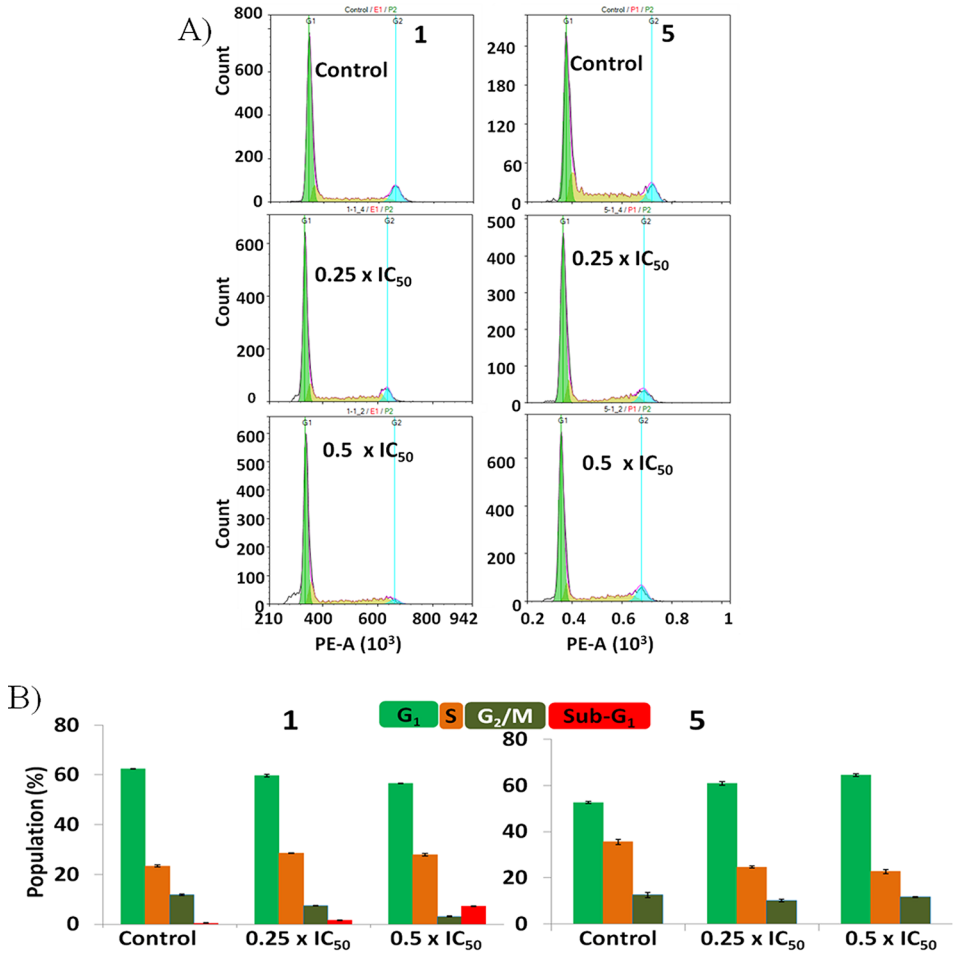

Figure 6. A549 cell cycle arrest by complexes **1** and **5** (concentrations used: 0.25 and 0.5 × IC_{50}) after 24 h at 310 K. Cell staining: PI. Control: cells untreated. (A) Cell cycle analysis examined by flow cytometry. (B) Bar chart showing cell populations in various cell cycles.

phase/S phase and G_1 phase, respectively. Additionally, significant apoptosis was induced by complexes **1** and **5** in A549 cancer cells. Complex **5** is more effective than complex **1** in the induction of ROS and apoptosis in A549 cells. This trend is consistent with their anticancer activity. Here, we conclude that the cytotoxicity of the complexes may be associated with the redox mechanism of action. This type of metal complex is worth further evaluation as chemotherapeutic agents.

EXPERIMENTAL SECTION

Materials. Unless otherwise noted, all manipulations were performed using standard Schlenk tube techniques under nitrogen atmosphere. The reagents $IrCl_3{\cdot}nH_2O$ (≥99% purity), hydrated $RuCl_3{\cdot}nH_2O$ (≥99% purity), octan-1-ol (≥99%), and NaCl (>99.999%), Nitric acid (72%), 2,3,4,5-tetramethyl-2-cyclopentenone (95%), 1,2,3,4,5-pentamethyl-cyclopentadiene (95%), butyllithium solution (1.6 M in hexane), 2,20-bis(diphenylphosphino)-1,10-binaphthyl (BINAP) (98%) 4-phenylbutan-1-ol, 3-phenylpropan-1-ol, α-terpinene were purchased from Sigma-Aldrich. $Cp^{xbiph}H$[18] were prepared as described. For the biological experiments, BSA, ctDNA, DMEM medium, fetal bovine serum, penicillin/streptomycin mixture, trypsin/EDTA, and phosphate-buffered saline (PBS) were purchased from Sangon Biotech. Testing compounds was dissolved in DMSO and diluted with the tissue culture medium before use.

Syntheses. The ^{1}H NMR (500 MHz, $CDCl_3$) peak integrals of $[(\eta^6\text{-bz-PA})RuCl_2]_2$ (**dimer 3**) are shown in Figure S9 in the Supporting Information. The ^{1}H NMR (500 MHz, DMSO) peak integrals of ligand 3′-(2,5-dihydrophenyl)propanol are shown in Figure S8, complexes **1**−**5** are shown in Figures S10−S14 in the Supporting Information.

Synthesis of Ligand 3′-(2,5-dihydrophenyl)propanol. A solution of 3-phenylpropan-1-ol (3.00 g, 22 mmol) in ethanol (10 mL) was slowly added to a stirred, cooled solution of ammonia (250 mL) at −78 °C. Small pieces of sodium were added to the reaction mixture until the blue colored persisted. During the addition of sodium, a small amount of ethanol was added to facilitate stirring. After the addition of sodium over the course of 4 h, the reaction mixture was left overnight to evaporate ammonia. The reaction was quenched carefully with ammonium chloride (sat., 100 mL), and extracted by DCM (3 × 25 mL). The combined organic layer was dried over magnesium sulfate, filtered and concentrated under reduced pressure to afford colorless oil (2.80 g, 92% yield). ^{1}H NMR (500 MHz, DMSO) δ 5.98 (d, J = 5.8 Hz, 1H), 5.74 (dd, J = 10.8, 5.7 Hz, 2H), 4.43 (t, J = 5.2 Hz, 1H), 3.42 (dd, J = 11.8, 6.3 Hz, 4H), 2.47−2.40 (m, 2H), 1.60 (dd, J = 10.0, 5.5 Hz, 2H), 1.48 (dd, J = 14.7, 6.7 Hz, 2H).

Synthesis of $[(\eta^6\text{-bz-PA})RuCl_2]_2$ (dimer 3). The ligand 3′-(2,5-dihydrophenyl)propanol (1.06 g,7.65 mmol) and $RuCl_3$ (400 mg, 1.53 mmol) was dissolved in methanol (60 mL) in a dry round-bottom flask equipped with stirrer and nitrogen atmosphere. The reaction mixture was heated to reflux for 16 h and subsequently cooled to −18 °C. The precipitate was filtered off, washed with cold ethanol and pentane (each 2 × 5 mL) and the red brown precipitate was dried in vacuo. Yield: 80% (377.2 mg, 0.61 mmol) ^{1}H NMR (500 MHz, $CDCl_3$) δ 7.32−7.23 (m, 2H), 7.23−7.08 (m, 3H), 3.64 (d, J = 6.5 Hz, 2H), 2.69 (d, J = 7.9 Hz, 2H), 1.91−1.85 (m, 2H), 1.77 (s, 1H).

Synthesis of Complexes 1−5. General method: The ligand 2,20-bis(diphenylphosphino)-1,10-binaphthyl (BINAP) (0.10 mmol) and

DOI: 10.1021/acs.inorgchem.7b01959
Inorg. Chem. XXXX, XXX, XXX−XXX

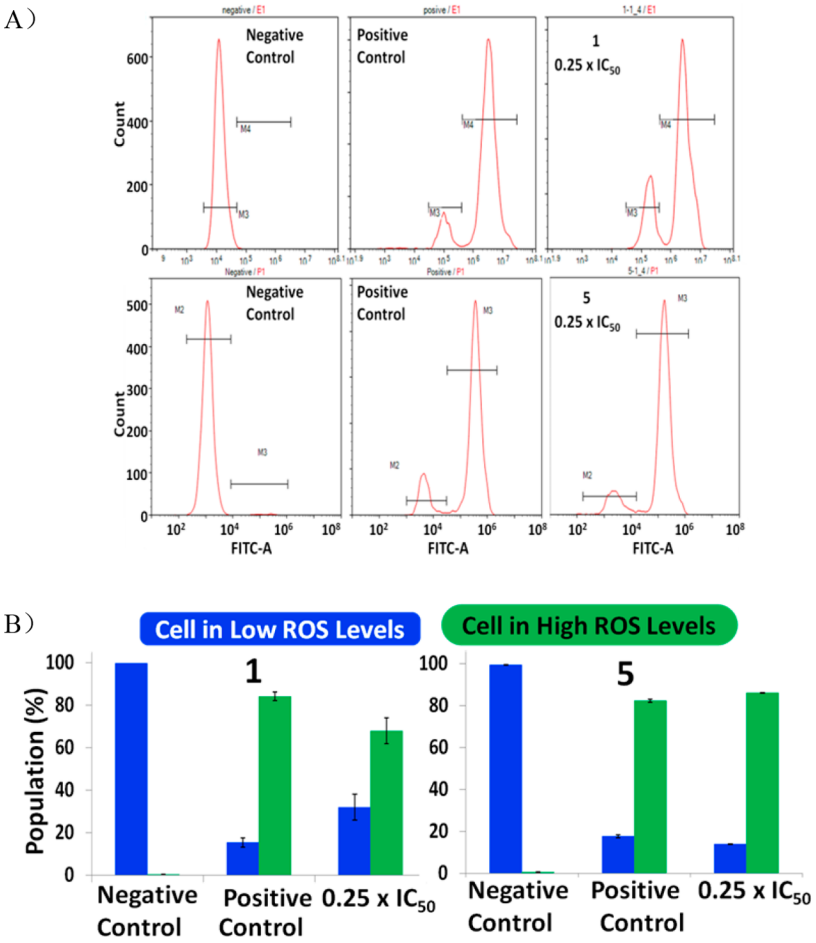

Figure 7. Induction of ROS levels in A549 cells by complexes **1** and **5** (concentrations used: 0.25 × IC_{50}) after 24 h at 310 K. (A) ROS levels analysis examined by flow cytometry. (B) Bar chart showing cell populations in high/low ROS levels.

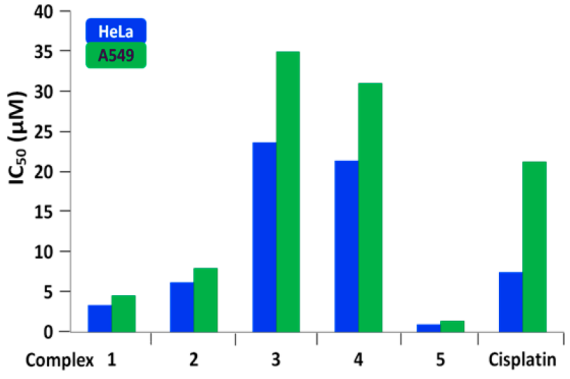

Figure 8. IC_{50} values of the complexes studied in this work toward A549 and HeLa cancer cells after an incubation of 24 h.

metal dimer $[(\eta^5\text{-Cp}^x)\text{IrCl}_2]_2$ or $[(\eta^6\text{-arene})\text{RuCl}_2]_2$ (0.05 mmol) was dissolved in methanol in a dry round-bottom flask equipped with stirrer and nitrogen atmosphere. After constant stirring for 4 h, NH_4PF_6 (0.2 mmol) was added at room temperature. The reaction mixture was stirred for 20 h at room temperature, and the progress of reaction was monitored by TLC. After complete conversion, methanol was removed under reduced pressure and product was dissolved in dichloromethane and filtered through Celite filtration funnel and recrystallized by slow diffusion of *n*-hexane in a concentrated solution of the compound in dichloromethane to obtain the corresponding complexes (**1**−**5**).

*$[(\eta^5\text{-Cp*})\text{Ir(P^P)Cl}]\text{PF}_6$ (**1**).* Yield: 61.73 mg, 54.6%. ^{1}H NMR (500 MHz, DMSO) δ 7.96 (d, J = 9.0 Hz, 1H), 7.89−7.74 (m, 3H), 7.73−7.62 (m, 7H), 7.51−7.42 (m, 2H), 7.40−7.30 (m, 2H), 7.27−6.97 (m, 11H), 6.96−6.81 (m, 4H), 6.50 (d, J = 8.7 Hz, 1H), 5.93 (d, J = 8.6 Hz, 1H), 1.12 (s, 15H). Anal. Calcd For $[(\eta^5\text{-Cp*})\text{Ir(P^P)Cl}]\text{PF}_6$ (1130.53): C, 57.37; H, 4.19; P, 8.22; Found: C, 57.45; H, 4.30; P, 8.35. MS: *m*/*z* 951.13 $[(\eta^5\text{-Cp*})\text{Ir(P^P)} + \text{H}]^+$.

*$[(\eta^5\text{-Cp}^{xbiph})\text{Ir(P^P)Cl}]\text{PF}_6$ (**2**).* Yield: 66.23 mg, 52.2%. ^{1}H NMR (500 MHz, DMSO) δ 7.96 (d, J = 10.0 Hz, 1H), 7.93−7.79 (m, 5H), 7.70 (d, J = 8.3 Hz, 4H), 7.66−7.52 (m, 5H), 7.46 (dd, J = 11.8, 7.7 Hz, 3H), 7.40−7.02 (m, 13H), 6.87 (ddd, J = 32.0, 18.2, 9.4 Hz, 8H), 6.53 (dd, J = 9.6, 3.6 Hz, 2H), 5.94 (d, J = 8.1 Hz, 1H), 1.76−1.58 (m, 6H), 0.97 (s, 3H), 0.79 (s, 3H). Anal. Calcd For $[(\eta^5\text{-Cp}^{xbiph})\text{Ir(P^P)Cl}]\text{PF}_6$ (1268.70): C, 61.54; H, 4.21; P, 7.32; Found: C, 61.65; H, 4.13; P, 7.41. MS: *m*/*z* 1089.30 $[(\eta^5\text{-Cp}^{xbiph})\text{Ir(P^P)} + \text{H}]^+$.

*$[(\eta^6\text{-bz-PA})\text{Ru(P^P)Cl}]\text{PF}_6$ (**3**).* Yield: 64.71 mg, 62.2%. ^{1}H NMR (500 MHz, DMSO) δ 7.86 (d, J = 8.8 Hz, 2H), 7.79 (d, J = 8.2 Hz, 1H), 7.76−7.56 (m, 9H), 7.52−7.13 (m, 12H), 6.99 (dt, J = 25.7, 8.5 Hz, 3H), 6.85 (t, J = 6.7 Hz, 2H), 6.41 (d, J = 8.7 Hz, 1H), 6.16 (d, J = 6.5 Hz, 1H), 5.84 (t, J = 6.1 Hz, 2H), 5.74 (dd, J = 9.6, 5.6 Hz, 1H), 4.86−4.80 (m, 1H), 4.59 (t, J = 6.5 Hz, 2H), 3.43−3.37 (m, 2H), 2.60 (dd, J = 10.4, 5.4 Hz, 1H), 2.36−2.29 (m, 1H), 1.71−1.60 (m, 2H). Anal. Calcd For $[(\eta^6\text{-bz-PA})\text{Ru(P^P)Cl}]\text{PF}_6$ (1040.35): C, 61.19; H, 4.26; O, 1.54; P, 8.93; Found: C, 61.06; H, 4.25; O, 1.59; P, 8.84. MS: *m*/*z* 859.95 $[(\eta^6\text{-bz-PA})\text{Ru(P^P)}]^+$.

*$[(\eta^6\text{-bz-BA})\ \text{Ru (P^P)Cl}]\text{PF}_6$ (**4**).* Yield: 58.20 mg, 55.2%. ^{1}H NMR (500 MHz, DMSO) δ 7.92−7.85 (m, 2H), 7.79 (d, J = 8.4 Hz, 1H), 7.69 (dd, J = 22.4, 7.9 Hz, 7H), 7.53−7.12 (m, 12H), 7.04−6.83 (m, 4H), 6.62−6.54 (m, 1H), 6.41 (d, J = 8.4 Hz, 1H), 6.16 (d, J = 6.3 Hz, 1H), 5.85 (dd, J = 10.0, 4.2 Hz, 2H), 5.75−5.68 (m, 1H), 4.85 (t, J =

DOI: 10.1021/acs.inorgchem.7b01959
Inorg. Chem. XXXX, XXX, XXX−XXX

5.0 Hz, 1H), 4.58 (d, J = 5.9 Hz, 2H), 4.39 (dt, J = 30.6, 5.0 Hz, 2H), 2.60−2.54 (m, 1H), 2.46−2.42 (m, 1H), 2.28 (dt, J = 10.3, 6.7 Hz, 2H), 1.60−1.50 (m, 2H), 1.46−1.37 (m, 2H). Anal. Calcd For [(η^6-bz-BA)Ru(P^P)Cl]PF_6 (1054.38): C, 61.51; H, 4.40; O, 1.52; P, 8.81; Found: C, 61.43; H, 4.36; O,1.58; P, 8.73; MS: *m/z* 874.98 [(η^6-bz-BA)Ru(P^P) + H]$^+$.

[(η^6 -p-cym)Ru(P^P)Cl]PF_6 (**5**). Yield: 60.54 mg 58.3%. ^{1}H NMR (500 MHz, DMSO) δ 7.96 (s, 2H), 7.79 (d, *J* = 8.6 Hz, 2H), 7.77−7.64 (m, 5H), 7.60 (t, *J* = 9.0 Hz, 2H), 7.48−7.09 (m, 9H), 7.02−6.91 (m, 2H), 6.90−6.85 (m, 1H), 6.84−6.73 (m, 2H), 6.35 (dd, *J* = 31.6, 7.9 Hz, 4H), 5.83 (d, *J* = 6.3 Hz, 2H), 5.77 (d, *J* = 9.1 Hz, 1H), 4.52 (d, *J* = 7.1 Hz, 2H), 4.32 (d, *J* = 4.1 Hz, 2H), 2.97−2.92 (m, 1H), 1.76 (s, 3H), 1.31 (d, *J* = 6.9 Hz, 3H), 0.95 (d, *J* = 6.7 Hz, 3H). Anal. Calcd For [(η^6-*p*-cym)Ru(P^P)Cl]PF_6 (1038.38): C, 62.46; H, 4.47; P, 8.95; Found: C, 62.45; H, 4.48; P, 8.93. MS: *m/z* 858.98 [(η^6-*p*-cym)Ru(P^P) + H]$^+$.

■ ASSOCIATED CONTENT

Supporting Information

The Supporting Information is available free of charge on the ACS Publications website at DOI: 10.1021/acs.inorgchem.7b01959.

Experimental details; Figures S1−S14; and Tables S1−S3 (PDF)

Accession Codes

CCDC 1562301−1562303 contain the supplementary crystallographic data for this paper. These data can be obtained free of charge via www.ccdc.cam.ac.uk/data_request/cif, or by emailing data_request@ccdc.cam.ac.uk, or by contacting The Cambridge Crystallographic Data Centre, 12 Union Road, Cambridge CB2 1EZ, UK; fax: +44 1223 336033.

■ AUTHOR INFORMATION

Corresponding Author

*E-mail: liuzheqd@163.com.

ORCID

Zhe Liu: 0000-0001-5796-4335

Notes

The authors declare no competing financial interest.

■ ACKNOWLEDGMENTS

We thank the National Natural Science Foundation of China (Grant No. 21671118) and the Taishan Scholars Program for support. We thank Dr Abraha Habtemariam for stimulating discussions.

■ REFERENCES

(1) Rosenberg, B.; Vancamp, L.; Trosko, J. E.; Mansour, V. H. Platinum compounds: a new class of potent antitumour agents. *Nature* **1969**, *222*, 385.

(2) Medici, S.; Peana, M.; Nurchi, V. M.; Lachowicz, J. I.; Crisponi, G.; Zoroddu, M. A. Noble metals in medicine: Latest advances. *Coord. Chem. Rev.* **2015**, *284*, 329−350.

(3) Johnstone, T. C.; Suntharalingam, K.; Lippard, S. J. The next generation of platinum drugs: targeted Pt (II) agents, nanoparticle delivery, and Pt (IV) prodrugs. *Chem. Rev.* **2016**, *116*, 3436−3486.

(4) Liu, Z.; Sadler, P. J. Organoiridium Complexes: Anticancer Agents and Catalysts. *Acc. Chem. Res.* **2014**, *47*, 1174−1185.

(5) Wang, X.; Wang, X.; Guo, Z. Functionalization of platinum complexes for biomedical applications. *Acc. Chem. Res.* **2015**, *48*, 2622−2631.

(6) Tian, M.; Li, J.; Zhang, S.; Guo, L.; He, X.; Kong, D.; Zhang, H.; Liu, Z. Half-sandwich ruthenium(ii) complexes containing N^N-chelated imino-pyridyl ligands that are selectively toxic to cancer cells. *Chem. Commun.* **2017**, *53*, 12810−12813.

(7) Leung, C.-H.; Zhong, H.-J.; Chan, D. S.-H.; Ma, D.-L. Bioactive iridium and rhodium complexes as therapeutic agents. *Coord. Chem. Rev.* **2013**, *257*, 1764−1776.

(8) Albada, B.; Metzler-Nolte, N. Organometallic−Peptide Bioconjugates: Synthetic Strategies and Medicinal Applications. *Chem. Rev.* **2016**, *116*, 11797−11839.

(9) Allardyce, C. S.; Dyson, P. J. Metal-based drugs that break the rules. *Dalton Trans.* **2016**, *45*, 3201−3209.

(10) Pröhl, M.; Schubert, U. S.; Weigand, W.; Gottschaldt, M. Metal complexes of curcumin and curcumin derivatives for molecular imaging and anticancer therapy. *Coord. Chem. Rev.* **2016**, *307*, 32−41.

(11) Sava, G.; Giraldi, T.; Mestroni, G.; Zassinovich, G. Antitumor effects of rhodium (I), iridium (I) and ruthenium (II) complexes in comparison with cis-dichlorodiammino platinum (II) in mice bearing Lewis lung carcinoma. *Chem.-Biol. Interact.* **1983**, *45*, 1−6.

(12) Messori, L.; Marcon, G.; Orioli, P.; Fontani, M.; Zanello, P.; Bergamo, A.; Sava, G.; Mura, P. Molecular structure, solution chemistry and biological properties of the novel [ImH][trans-$IrCl_4$(Im)(DMSO)],(I) and of the orange form of [$(DMSO)_2$H][trans-$IrCl_4(DMSO)_2$],(II), complexes. *J. Inorg. Biochem.* **2003**, *95*, 37−46.

(13) Hearn, J. M.; Romero-Canelón, I.; Qamar, B.; Liu, Z.; Hands-Portman, I.; Sadler, P. J. Organometallic iridium (III) anticancer complexes with new mechanisms of action: NCI-60 screening, mitochondrial targeting, and apoptosis. *ACS Chem. Biol.* **2013**, *8*, 1335−1343.

(14) Novohradsky, V.; Zerzankova, L.; Stepankova, J.; Kisova, A.; Kostrhunova, H.; Liu, Z.; Sadler, P. J.; Kasparkova, J.; Brabec, V. A dual-targeting, apoptosis-inducing organometallic half-sandwich iridium anticancer complex. *Metallomics* **2014**, *6*, 1491−1501.

(15) Liu, Z.; Romero-Canelón, I.; Qamar, B.; Hearn, J. M.; Habtemariam, A.; Barry, N. P.; Pizarro, A. M.; Clarkson, G. J.; Sadler, P. J. The potent oxidant anticancer activity of organoiridium catalysts. *Angew. Chem., Int. Ed.* **2014**, *53*, 3941−3946.

(16) Li, Y.; Tan, C. P.; Zhang, W.; He, L.; Ji, L. N.; Mao, Z. W. Phosphorescent iridium(III)-bis-N-heterocyclic carbene complexes as mitochondria-targeted theranostic and photodynamic anticancer agents. *Biomaterials* **2015**, *39*, 95−104.

(17) Tabrizi, L.; Chiniforoshan, H. Designing new iridium (III) arene complexes of naphthoquinone derivatives as anticancer agents: a structure−activity relationship study. *Dalton Trans.* **2017**, *46*, 2339−2349.

(18) Wang, C.; Liu, J.; Tian, Z.; Tian, M.; Tian, L.; Zhao, W.; Liu, Z. Half-sandwich iridium N-heterocyclic carbene anticancer complexes. *Dalton Trans.* **2017**, *46*, 6870−6883.

(19) He, L.; Tan, C. P.; Ye, R. R.; Zhao, Y. Z.; Liu, Y. H.; Zhao, Q.; Ji, L. N.; Mao, Z. W. Theranostic Iridium (III) Complexes as One-and Two-Photon Phosphorescent Trackers to Monitor Autophagic Lysosomes. *Angew. Chem., Int. Ed.* **2014**, *53*, 12137−12141.

(20) Sudding, L. C.; Payne, R.; Govender, P.; Edafe, F.; Clavel, C. M.; Dyson, P. J.; Therrien, B.; Smith, G. S. Evaluation of the invitro anticancer activity of cyclometalated half-sandwich rhodium and iridium complexes coordinated to naphthaldimine-based poly-(propyleneimine) dendritic scaffolds. *J. Organomet. Chem.* **2014**, *774*, 79−85.

(21) Lucas, S. J.; Lord, R. M.; Basri, A. M.; Allison, S. J.; Phillips, R. M.; Blacker, A. J.; McGowan, P. C. Increasing anti-cancer activity with longer tether lengths of group 9 Cp* complexes. *Dalton Trans.* **2016**, *45*, 6812−6815.

(22) Ruiz, J.; Vicente, C.; de Haro, C. n.; Bautista, D. Novel bis-C, N-cyclometalated iridium (III) thiosemicarbazide antitumor complexes: interactions with human serum albumin and DNA, and Inhibition of cathepsin B. *Inorg. Chem.* **2013**, *52*, 974−982.

(23) Li, Y.; Tan, C.-P.; Zhang, W.; He, L.; Ji, L.-N.; Mao, Z.-W. Phosphorescent iridium (III)-bis-N-heterocyclic carbene complexes as mitochondria-targeted theranostic and photodynamic anticancer agents. *Biomaterials* **2015**, *39*, 95−104.

DOI: 10.1021/acs.inorgchem.7b01959
Inorg. Chem. XXXX, XXX, XXX−XXX

(24) Wilbuer, A.; Vlecken, D. H.; Schmitz, D. J.; Kräling, K.; Harms, K.; Bagowski, C. P.; Meggers, E. Iridium complex with antiangiogenic properties. *Angew. Chem., Int. Ed.* **2010**, *49*, 3839−3842.
(25) Gras, M.; Therrien, B.; Süss-Fink, G.; Casini, A.; Edafe, F.; Dyson, P. J. Anticancer activity of new organo-ruthenium, rhodium and iridium complexes containing the 2-(pyridine-2-yl) thiazole N, N-chelating ligand. *J. Organomet. Chem.* **2010**, *695*, 1119−1125.
(26) Geldmacher, Y.; Kitanovic, I.; Alborzinia, H.; Bergerhoff, K.; Rubbiani, R.; Wefelmeier, P.; Prokop, A.; Gust, R.; Ott, I.; Wölfl, S.; Sheldrick, W. S. Cellular selectivity and biological impact of cytotoxic rhodium(III) and iridium(III) complexes containing methyl-substituted phenanthroline ligands. *ChemMedChem* **2011**, *6*, 429−439.
(27) Schäfer, S.; Sheldrick, W. S. Coligand Tuning of the DNA Binding Properties of Half-Sandwich Organometallic Intercalators: Influence of Polypyridyl (pp) and Monodentate Ligands (L = Cl, (NH2)2CS, (NMe2)2CS) on the Intercalation of (η5-pentamethylcyclopentadienyl)-iridium(III)-dipyridoquinoxaline and -dipyridophenazine Complexes. *J. Organomet. Chem.* **2007**, *692*, 1300−1309.
(28) Liu, Z.; Habtemariam, A.; Pizarro, A. M.; Fletcher, S. A.; Kisova, A.; Vrana, O.; Salassa, L.; Bruijnincx, P. C. A.; Clarkson, G. J.; Brabec, V.; Sadler, P. J. Organometallic Half-Sandwich Iridium Anticancer Complexes. *J. Med. Chem.* **2011**, *54*, 3011−3026.
(29) Liu, Z.; Salassa, L.; Habtemariam, A.; Pizarro, A. M.; Clarkson, G. J.; Sadler, P. J. Contrasting Reactivity and Cancer Cell Cytotoxicity of Isoelectronic Organometallic Iridium(III) Complexes. *Inorg. Chem.* **2011**, *50*, 5777−5783.
(30) Liu, Z.; Habtemariam, A.; Pizarro, A.; Clarkson, G. J.; Sadler, P. J. Organometallic Iridium(III) Cyclopentadienyl Anticancer Complexes Containing C,N-Chelating Ligands. *Organometallics* **2011**, *30*, 4702−4710.
(31) Reedijk, J. Metal-Ligand Exchange Kinetics in Platinum and Ruthenium Complexes. *Platinum Met. Rev.* **2008**, *52*, 2−11.
(32) Clarke, M. J. Ruthenium chemistry pertaining to the design of anticancer agents. In *Ruthenium and Other Non-Platinum Metal Complexes in Cancer Chemotherapy*; Springer: 1989; pp 25−39.
(33) Srivastava, S. C.; Mausner, L. F.; Clarke, M. J. Radioruthenium-labeled compounds for diagnostic tumor imaging. In *Ruthenium and Other Non-Platinum Metal Complexes in Cancer Chemotherapy*; Springer: 1989; pp 111−149.
(34) Sava, G.; Pacor, S.; Mestroni, G.; Alessio, E. Na[trans -RuCl 4 (DMSO)Im], a metal complex of ruthenium with antimetastatic properties. *Clin. Exp. Metastasis* **1992**, *10*, 273−280.
(35) Berger, M. R.; Garzon, F. T.; Keppler, B. K.; Schmähl, D. Efficacy of new ruthenium complexes against chemically induced autochthonous colorectal carcinoma in rats. *Anticancer Res.* **1989**, *9*, 761−765.
(36) Zeng, L.; Gupta, P.; Chen, Y.; Wang, E.; Ji, L.; Chao, H.; Chen, Z.-S. The development of anticancer ruthenium(ii) complexes: from single molecule compounds to nanomaterials. *Chem. Soc. Rev.* **2017**, *46*, 5771−5804.
(37) Aird, R.; Cummings, J.; Ritchie, A.; Muir, M.; Morris, R.; Chen, H.; Sadler, P.; Jodrell, D. In vitro and in vivo activity and cross resistance profiles of novel ruthenium (II) organometallic arene complexes in human ovarian cancer. *Br. J. Cancer* **2002**, *86*, 1652.
(38) Scolaro, C.; Bergamo, A.; Brescacin, L.; Delfino, R.; Cocchietto, M.; Laurenczy, G.; Geldbach, T. J.; Sava, G.; Dyson, P. J. In vitro and in vivo evaluation of ruthenium (II)− arene PTA complexes. *J. Med. Chem.* **2005**, *48*, 4161−4171.
(39) Almodares, Z.; Lucas, S. J.; Crossley, B. D.; Basri, A. M.; Pask, C. M.; Hebden, A. J.; Phillips, R. M.; McGowan, P. C. Rhodium, Iridium, and Ruthenium Half-Sandwich Picolinamide Complexes as Anticancer Agents. *Inorg. Chem.* **2014**, *53*, 727−736.
(40) Habtemariam, A.; Melchart, M.; Fernández, R.; Parsons, S.; Oswald, I. D. H.; Parkin, A.; Fabbiani, F. P. A.; Davidson, J. E.; Dawson, A.; Aird, R. E.; Jodrell, D. I.; Sadler, P. J. Structure−Activity Relationships for Cytotoxic Ruthenium(II) Arene Complexes Containing N,N-, N,O-, and O,O-Chelating Ligands. *J. Med. Chem.* **2006**, *49*, 6858−6868.
(41) Liu, H.-K.; Sadler, P. J. Metal complexes as DNA intercalators. *Acc. Chem. Res.* **2011**, *44*, 349−359.
(42) Albani, B. A.; Peña, B.; Leed, N. A.; De Paula, N. A.; Pavani, C.; Baptista, M. S.; Dunbar, K. R.; Turro, C. Marked improvement in photoinduced cell death by a new tris-heteroleptic complex with dual action: Singlet oxygen sensitization and ligand dissociation. *J. Am. Chem. Soc.* **2014**, *136*, 17095−17101.
(43) Liu, Z.; Lebrun, V.; Kitanosono, T.; Mallin, H.; Köhler, V.; Häussinger, D.; Hilvert, D.; Kobayashi, S.; Ward, T. R. Upregulation of an Artificial Zymogen by Proteolysis. *Angew. Chem., Int. Ed.* **2016**, *55*, 11587−11590.
(44) Guo, L.; Jing, X.; Xiong, S.; Liu, W.; Liu, Y.; Liu, Z.; Chen, C. Influences of Alkyl and Aryl Substituents on Iminopyridine Fe (II)-and Co (II)-Catalyzed Isoprene Polymerization. *Polymers* **2016**, *8*, 389.
(45) Ludwig, G.; Mijatović, S.; Ranđelović, I.; Bulatović, M.; Miljković, D.; Maksimović-Ivanić, D.; Korb, M.; Lang, H.; Steinborn, D.; Kaluđerović, G. N. Biological activity of neutral and cationic iridium (III) complexes with κP and κP, κS coordinated Ph 2 PCH 2 S (O) x Ph (x= 0−2) ligands. *Eur. J. Med. Chem.* **2013**, *69*, 216−222.
(46) Wang, T.; Wang, W.; Lyu, Y.; Xiong, K.; Li, C.; Zhang, H.; Zhan, Z.; Jiang, Z.; Ding, Y. Porous Rh/BINAP polymers as efficient heterogeneous catalysts for asymmetric hydroformylation of styrene: Enhanced enantioselectivity realized by flexible chiral nanopockets. *Chinese. J. Catal.* **2017**, *38*, 691−698.
(47) Reiner, T.; Waibel, M.; Marziale, A. N.; Jantke, D.; Kiefer, F. J.; Fässler, T. F.; Eppinger, J. η6-Arene complexes of ruthenium and osmium with pendant donor functionalities. *J. Organomet. Chem.* **2010**, *695*, 2667−2672.
(48) Jensen, S. B.; Rodger, S. J.; Spicer, M. D. Facile preparation of η 6 - p -cymene ruthenium diphosphine complexes. Crystal structure of [(η 6 - p -cymene)Ru(dppf)Cl]PF 6. *J. Organomet. Chem.* **1998**, *556*, 151−158.
(49) Cheung, F. K.; Lin, C.; Minissi, F.; Lorente Criville, A.; Graham, M. A.; Fox, D. J.; Wills, M. An Investigation into the Tether Length and Substitution Pattern of Arene-Substituted Complexes for Asymmetric Transfer Hydrogenation of Ketones. *Org. Lett.* **2007**, *9*, 4659−4662.
(50) Li, L.; Brennessel, W. W.; Jones, W. D. An Efficient Low-Temperature Route To Polycyclic Isoquinoline Salt Synthesis via C−H Activation with [Cp* MCl2] 2 (M= Rh, Ir). *J. Am. Chem. Soc.* **2008**, *130*, 12414−12419.
(51) Wirth, S.; Rohbogner, C. J.; Cieslak, M.; Kazmierczak-Baranska, J.; Donevski, S.; Nawrot, B.; Lorenz, I.-P. Rhodium(III) and iridium(III) complexes with 1,2-naphthoquinone-1-oximate as a bidentate ligand: synthesis, structure, and biological activity. *JBIC, J. Biol. Inorg. Chem.* **2010**, *15*, 429−440.
(52) Schäfer, S.; Sheldrick, W. S. Coligand tuning of the DNA binding properties of half-sandwich organometallic intercalators: Influence of polypyridyl (pp) and monodentate ligands (L = Cl, (NH2)2CS, (NMe2)2CS) on the intercalation of (η5-pentamethylcyclopentadienyl)-iridium(III)- dipyridoquinoxaline and -dipyridophenazine complexes. *J. Organomet. Chem.* **2007**, *692*, 1300−1309.
(53) Ganeshpandian, M.; Loganathan, R.; Suresh, E.; Riyasdeen, A.; Akbarsha, M. A.; Palaniandavar, M. New ruthenium(ii) arene complexes of anthracenyl-appended diazacycloalkanes: effect of ligand intercalation and hydrophobicity on DNA and protein binding and cleavage and cytotoxicity. *Dalton Trans.* **2014**, *43*, 1203−1219.
(54) Gupta, G.; Sharma, G.; Koch, B.; Park, S.; Lee, S. S.; Kim, J. Syntheses, characterization and molecular structures of novel Ru(ii), Rh(iii) and Ir(iii) complexes and their possible roles as antitumour and cytotoxic agents. *New J. Chem.* **2013**, *37*, 2573−2581.
(55) Ghose, A. K.; Viswanadhan, V. N.; Wendoloski, J. J. A Knowledge-Based Approach in Designing Combinatorial or Medicinal Chemistry Libraries for Drug Discovery. 1. A Qualitative and Quantitative Characterization of Known Drug Databases. *J. Comb. Chem.* **1999**, *1*, 55−68.
(56) Li, L.-J.; Yan, Q.-Q.; Liu, G.-J.; Yuan, Z.; Lv, Z.-H.; Fu, B.; Han, Y.-J.; Du, J.-L. Synthesis characterization and cytotoxicity studies of platinum (II) complexes with reduced amino pyridine schiff base and

DOI: 10.1021/acs.inorgchem.7b01959
Inorg. Chem. XXXX, XXX, XXX−XXX

its derivatives as ligands. *Biosci., Biotechnol., Biochem.* **2017**, *81*, 1081−1089.
(57) Umadevi, C.; Kalaivani, P.; Puschmann, H.; Murugan, S.; Mohan, P.; Prabhakaran, R. Substitutional impact on biological activity of new water soluble Ni (II) complexes: Preparation, spectral characterization, X-ray crystallography, DNA/protein binding, antibacterial activity and in vitro cytotoxicity. *J. Photochem. Photobiol., B* **2017**, *167*, 45−57.
(58) Skladanowski, A.; Bozko, P.; Sabisz, M. DNA Structure and Integrity Checkpoints During the Cell Cycle and Their Role in Drug Targeting and Sensitivity of Tumor Cells to Anticancer Treatment. *Chem. Rev.* **2009**, *109*, 2951−2973.
(59) Liu, Z.; Deeth, R. J.; Butler, J. S.; Habtemariam, A.; Newton, M. E.; Sadler, P. J. Reduction of Quinones by NADH Catalyzed by Organoiridium Complexes. *Angew. Chem., Int. Ed.* **2013**, *52*, 4194−4197.
(60) Steckhan, E.; Herrmann, S.; Ruppert, R.; Dietz, E.; Frede, M.; Spika, E. Analytical study of a series of substituted (2, 2′-bipyridyl)(pentamethylcyclopentadienyl) rhodium and-iridium complexes with regard to their effectiveness as redox catalysts for the indirect electrochemical and chemical reduction of $NAD(P)^+$. *Organometallics* **1991**, *10*, 1568−1577.
(61) Betanzos-Lara, S.; Liu, Z.; Habtemariam, A.; Pizarro, A. M.; Qamar, B.; Sadler, P. J. Organometallic Ruthenium and Iridium Transfer-Hydrogenation Catalysts Using Coenzyme NADH as a Cofactor. *Angew. Chem., Int. Ed.* **2012**, *51*, 3897−3900.
(62) Muhammad, N.; Guo, Z. Metal-based anticancer chemotherapeutic agents. *Curr. Opin. Chem. Biol.* **2014**, *19*, 144−153.
(63) Zhou, Y.; Hileman, E. O.; Plunkett, W.; Keating, M. J.; Huang, P. Free radical stress in chronic lymphocytic leukemia cells and its role in cellular sensitivity to ROS-generating anticancer agents. *Blood* **2003**, *101*, 4098−4104.
(64) Romero-Canelón, I.; Mos, M.; Sadler, P. J. Enhancement of selectivity of an organometallic anticancer agent by redox modulation. *J. Med. Chem.* **2015**, *58*, 7874−7880.

DOI: 10.1021/acs.inorgchem.7b01959
Inorg. Chem. XXXX, XXX, XXX−XXX